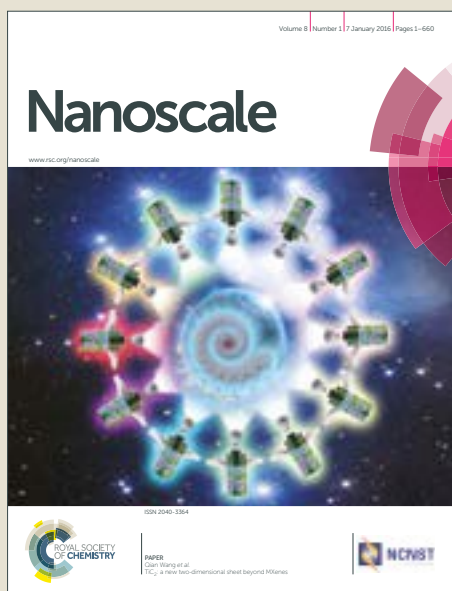


# Nanoscale

Accepted Manuscript



This article can be cited before page numbers have been issued, to do this please use: R. Xie, C. Batchelor-McAuley, N. P. Young and R. G. Compton, *Nanoscale*, 2019, DOI: 10.1039/C8NR09172B.



This is an Accepted Manuscript, which has been through the Royal Society of Chemistry peer review process and has been accepted for publication.

Accepted Manuscripts are published online shortly after acceptance, before technical editing, formatting and proof reading. Using this free service, authors can make their results available to the community, in citable form, before we publish the edited article. We will replace this Accepted Manuscript with the edited and formatted Advance Article as soon as it is available.

You can find more information about Accepted Manuscripts in the [author guidelines](#).

Please note that technical editing may introduce minor changes to the text and/or graphics, which may alter content. The journal's standard [Terms & Conditions](#) and the ethical guidelines, outlined in our [author and reviewer resource centre](#), still apply. In no event shall the Royal Society of Chemistry be held responsible for any errors or omissions in this Accepted Manuscript or any consequences arising from the use of any information it contains.

# Electrochemical Impacts Complement Light Scattering Techniques for In-situ Nanoparticle Sizing

View Article Online  
DOI: 10.1039/C8NR09172B

*Ruochen Xie, Christopher Batchelor-McAuley, Neil P. Young and Richard G Compton\**

\* Corresponding author: Richard G. Compton. Department of Chemistry, Physical & Theoretical Chemistry Laboratory, Oxford University, South Parks Road, Oxford, OX1 3QZ, United Kingdom

Email: richard.compton@chem.ox.ac.uk. Tel: +44(0)1865275 957 Fax: +44(0)1865275410

## Abstract

We show that the electrochemical particle-impact technique (or ‘nano-impacts’) complements light scattering techniques for sizing both mono- and poly-disperse nanoparticles. It is found that established techniques – Dynamic Light Scattering (DLS) and Nanoparticle Tracking Analysis (NTA) – can accurately measure the diameters of ‘30 nm’ silver particles assuming spherical shapes, but are unable to accurately size a smaller ‘20 nm’ sample. In contrast, nano-impacts have a high accuracy (< 5% error in effective diameters) and are able to size both individual ‘20 nm’ and ‘30 nm’ silver NPs in terms of the number of constituent atoms. Further study of a ‘20 nm and 30 nm’ bimodal sample shows that the electrochemical technique resolves the two very similar sizes well, demonstrating accurate sizing regardless of particle size polydispersity, whereas due to inherent limitations of light scattering measurements this is not possible for DLS and NTA. Electrochemical sizing is concluded to offer significant attractions over light scattering methods.

## 1. Introduction

View Article Online  
DOI: 10.1039/C8NR09172B

Size controls many physical and chemical properties of nanomaterials, including luminescence, catalytic activity and toxicity.<sup>1-3</sup> For nanoparticles (NPs) with well-defined geometries such as spheres or prisms, the particle size can be defined by simple parameters. However, most NPs exhibit a degree of irregularity in their shapes. Moreover, no NP samples contain truly monodisperse particles, which dictates a size distribution for the description of particle populations. Moreover, efficient and precise sizing measurements of multimodal NP samples are desirable.<sup>4, 5</sup> These present difficulties in the accurate determination of NP sizes for current analytical techniques based on light scattering.

Dynamic Light Scattering (DLS) and Nanoparticle Tracking Analysis (NTA) have been widely used as established techniques for size measurements of NPs in many fields involving environmental and biological studies.<sup>6, 7</sup> Both light scattering techniques provide an *in situ* measurement of hydrodynamic radii of the NPs which are assumed spherical. The measured quantities are often larger than the geometric radii. However, while it is well known that DLS can only resolve particles that differ in diameter by at least a factor of 3,<sup>7</sup> many studies have shown that for metal NPs such as silver and gold, the technique tend to yield markedly larger (> 50%) diameters than expected when the particle sizes are small (e.g. < 30 nm).<sup>3, 8-12</sup> The latter may in part reflect the significant effects of operational procedures on the measurement accuracy.<sup>13</sup> For NTA, due to individual visualization of particles, the technique has a much better size resolution (of two particles with less than 0.5 fold difference in diameter),<sup>7</sup> but for small NPs it may have difficulty in detecting them depending on the optical properties of the NPs and the type of laser used owing to a fourth-power dependence of scattered light intensity on the wavelength of incident light.<sup>14</sup> In addition to improvements in the mature techniques themselves, this poses a question of how can these small

NPs, especially when examined as polydisperse samples, be better sized using other sizing alternatives?

View Article Online  
DOI: 10.1039/C8NR09172B

Among all the NP sizing techniques, transmission electron microscopy (TEM) offers excellent resolution in defining the particle size and shape based on projection images. However, TEM only measures samples in high definition when the particles are completely dry and clean. In addition, a recent study using electron tomography shows that even for some of the particles appearing to be almost spherical there is still an overestimation of *ca.* 8% in particle diameter.<sup>15</sup> An emerging technique in recent years, electrochemical particle-impact technique (or 'nano-impacts'), has been demonstrated as a volume-based sizing technique for many kinds of NPs such as metals,<sup>16</sup> organics<sup>17</sup> and polymeric NPs<sup>18</sup> using appropriate electrolytes and applied potentials. Recent developments of the nano-impact method have been reviewed.<sup>19-21</sup> In particular, a systematic quantitative methodology has been established for the technique in sizing NPs.<sup>22</sup> In this work, we aim to compare the electrochemical alternative with the light scattering techniques in sizing small NPs mainly in terms of measurement accuracy. To this end, the nominally '20 nm' and '30 nm'-diameter silver particles are selected and studied in both their individual dispersions as well as a bimodal sample. Insights into the strengths and limitations of the involved techniques are consequently obtained.

## 2. Experimental Section

**Chemical reagents.** Citrate-capped '20 nm' silver nanoparticles (Ag NPs) were synthesized following a seeded growth method as a 0.13 mg/mL particle dispersion containing 2 mM of

sodium citrate.<sup>23</sup> The '20 nm' diameter and quasi-spherical shapes have been characterized by high-resolution SEM previously.<sup>24</sup> The '30 nm' silver nanoparticle suspension (NanoXact, 0.02 mg/mL silver, 2 mM sodium citrate) was purchased from NanoComposix, USA. Potassium Chloride ( $\geq 99.0\%$ ) was obtained from Sigma-Aldrich, and tri-sodium citrate (99.0%) from British Drug Houses. Solutions were prepared using deionized water (Millipore) with a resistivity of close to 18.2 M $\Omega$  cm at 298 K.

View Article Online  
DOI: 10.1039/C8NR09172B

**Electrochemical-impacts.** The nano-impact (or NI) experiments of both individual ('20 nm' and '30 nm') and mixed sizes were performed using an in-house low noise potentiostat as described previously.<sup>25</sup> Briefly, a low noise current amplifier (LCA-4K-1G, FEMTO Messtechnik GmbH, Germany) was used and filtered using two cascaded analogue RC-filters at 2K Hz. The filtered signal was then digitized at 100 kS s<sup>-1</sup> via a USB data acquisition device (USB-6003, National Instruments, Texas, US). The low-pass digital filter was set to 100 Hz. The filter design used in this work has been demonstrated to conserve the overall charge transferred in such nano-impact events.<sup>25, 26</sup> Current spikes were identified and analysed using a script written in Python 3.5.

The electrochemical measurements were carried out using a lab-built three-electrode system in a Faraday cage with temperature control at 25 °C. A 33  $\mu$ m diameter<sup>27</sup> carbon disc electrode (IJ Cambria Scientific Ltd, UK) was used as the working electrode. A leakless Ag/AgCl (in 3.0 M KCl, eDAQ) electrode was used as the reference electrode (+ 0.210 V vs. SHE), and a 0.5  $\times$  4  $\times$  8 mm<sup>3</sup> platinum mesh (Goodfellow, Cambridge, UK) as the counter electrode. The two silver particle dispersions, '20 nm' and '30 nm', were diluted and mixed with potassium chloride solution to a same particle concentration of 6 pM and 20 mM of KCl. The bimodal sample of '20 + 30 nm' was obtained by physically mixing the two stock individual samples with the chloride and citrate

solution in a ratio that results in equal particle concentrations of 6 pM and 1.8 mM of citrate, 20 mM of KCl. Then chronoamperometry, with a step potential of + 0.80 V vs. Ag/AgCl for 60 seconds per scan, was performed to detect the particle impacts at the working electrode immersed in the three dispersions described above. The carbon microdisc electrode was polished between each scan with 0.3, 0.05  $\mu\text{m}$  sized alumina in sequence and rinsed with deionized water.

**Dynamic Light Scattering.** The '20 nm' and '30 nm' particle diameter distributions with a concentration of 24 pM in 1.8 mM citrate were measured using a Nano ZS zetasizer system (Malvern Instruments). Measurement conditions mainly includes an irradiation wavelength of 632.8 nm (He laser) at a fixed backscatter angle of 173°, an equilibration time of 120 s, a measurement temperature of 298 K, a viscosity of 0.89 cP and refractive index of 1.3325 (of deionized water).<sup>28</sup> Prior to the measurement, the silver dispersions were filtered through a 0.22  $\mu\text{m}$  polyvinylidene fluoride (PVDF) membrane. Three measurements of 10-20 scans each were performed for each sample in general purpose algorithm (with normal resolution). A forward scattering angle of 13° and a multiple narrow algorithm (with high resolution) was also attempted.

**Nanoparticle Tracking Analysis.** Nanoparticle Tracking Analysis (NTA) was performed using a NanoSight LM10 (NanoSight, UK), equipped with a sample chamber with a 405 nm or 642 laser. The samples were diluted to a concentration of *ca.* 1 pM and injected in the sample chamber with sterile syringes (BsD Discardit II, New Jersey, USA). All measurements were performed for five times at a temperature of  $23.0 \pm 1.0$  °C. The samples were measured for 60 s with automatic exposure settings at 30 frames per second. The software used for video capture and data analysis was NTA 2.3.

**Transmission Electron Microscopy.** The nominally '20 and 30 nm' silver nanoparticles were imaged by transmission electron microscopy (TEM) using a JEOL JEM-3000F instrument with an accelerating voltage of 300 kV. Imaging magnification was 120 to 300 kx. Samples were prepared by drop-casting the nanoparticle suspensions (diluted 1/10 fold of the original stock suspension to 0.013 mg/mL Ag NPs, 0.2 mM sodium citrate for the '20 nm' particles; as-received 0.02 mg/mL Ag NPs, 2 mM sodium citrate for the '30 nm' particles) onto carbon grids (Agar Scientific) and allowing these to dry in air. Size information was subsequently extracted using ImageJ software.

View Article Online  
DOI: 10.1039/C8NR09172B

### 3. Results and discussion

The diameters of Ag NPs were first measured using TEM to provide values of the diameters for the individual '20 nm' and '30 nm' samples. Next, to present how accurately the established *in situ* methods can size these small particles, the two NP dispersions were measured by NTA and DLS. As reported below, we find that both light scattering techniques measured diameters of 5-20% larger for the '30 nm' particles than the TEM reference values yet over 50% larger for the '20 nm' sample. To approach the question of how the electrochemical alternative performs in sizing these small NPs, the nano-impact (or NI) method is then applied to study the individual samples and further to investigate a mixed sample of the two particle sizes. The electrochemical measurements show an accuracy of within 5% error of the TEM results for both individual and the bimodal sizing. Advantages of the nano-impact methodology over the other involved techniques are discussed.

#### 3.1. TEM analysis

TEM measurements were conducted for the silver NPs of both sizes. With high magnification of 120 to 300 kx, TEM images of '20 nm' (N=123) and '30 nm' (N=110) silver particles were obtained

as shown in Figure 1. It was observed that for both sizes most particles appear to be quasi-spherical. As such, 2D areas of the particles were measured using a freehand tool for outlining the particle boundaries<sup>29</sup> and then converted to effective geometric diameters, where the median values were measured as  $18.5 \pm 0.3$  nm and  $28.9 \pm 0.5$  nm for later direct comparison (See Table 1). The standard deviations represent the measurement uncertainty as from defining the particle boundaries in the TEM images and were determined as 0.3 and 0.5 nm on average for the '20 nm' and '30 nm' particles respectively. This error estimation is described in detail in the SI Section S1. This measurement uncertainty is of importance as compared to the other errors of typically some 0.5 nm (Table 1) in diameter obtained from reproducibility and would be more significant for images with lower resolution.

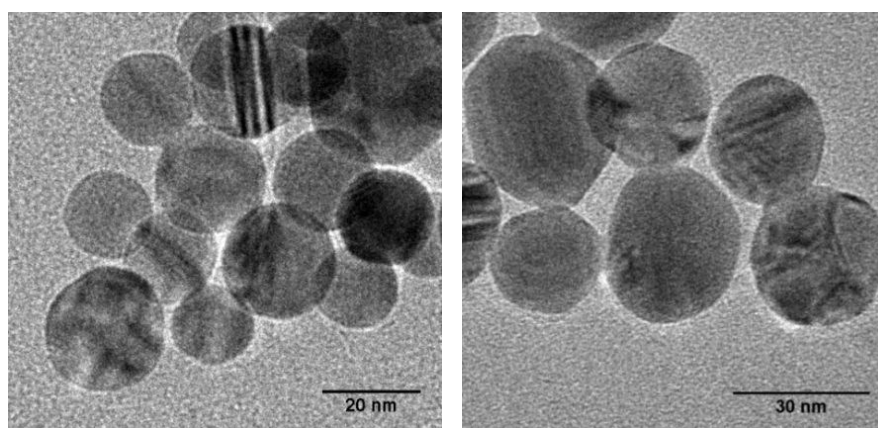


**Figure 1.** TEM images of the '20 nm' (left) and '30 nm' (right)-diameter silver particles.

### 3.2. Light scattering measurements

NTA measurements were performed to measure the diameters of the NPs in dispersions. This *in situ* technique uses a laser as the light source, illuminating the suspended particles to scatter lights and allow individual entities to be visualized, tracked and analyzed. According to the Rayleigh Scattering theory, the scattered light intensity of NPs is inversely proportional to the fourth power of the wavelength of the laser.<sup>14</sup> Moreover, the light scattering of the metallic NPs are significantly affected by surface plasmon resonance (SPR). As such, the type of laser is crucial for these very



small particles to be detected in the first place. Herein, a 642 nm and a 405 nm laser were used to study the two samples. It is noted that the 642 nm laser is commonly used in NanoSight instruments while the wavelength of 405 nm, which is also commercially available, is near the SPR of the silver NPs. Diameter distributions (Figure 2) and the median diameters (Table 1) were obtained; the number of tracks per measurement was also recorded to represent the data statistics.

When using the 642 nm laser, few '30 nm' particles were observed in the microscopic view and consequently around 150 tracks per measurement were recorded with a measured median diameter as large as  $49.6 \pm 2.5$  nm. Then using a 405 nm laser, approximately 18,000 tracks per measurement were measured and the diameter distribution of the '30 nm' particles is in overall good agreement with the TEM results though slightly larger (5%) than the reference values, considering that a hydrodynamic radius is often larger than the geometric radius of a particle. The significantly larger number of detected particles is due to far more scattered rays measured when using the shorter-wavelength laser.<sup>14</sup> For the smaller '20 nm' particles, changing to use the 405 nm laser led the number of tracks to increase from *ca.* 100 to 5000 per measurement. Accordingly, the results of the median diameters showed, a decrease from  $44.2 \pm 1.6$  nm to  $27.8 \pm 0.4$  nm that is, however, still much larger (9 nm) than that of the TEM results. Although the technique measures hydrodynamic diameters, this 50% discrepancy is too significant to render the result accurate. It follows that the NTA is able to accurately measure the '30 nm' silver particles with the 405 nm laser but unable to do so for the smaller '20 nm' sample.

Next, the other light scattering technique DLS (equipped with a 633 nm laser) was used to size the particles. The technique measures the intensity fluctuation of scattered light of particle ensembles without the requirement of them being visualized individually as in NTA,<sup>7</sup> and thus is likely more

sensitive in sizing small NPs. The intensity diameter distributions were obtained and herein converted to cumulative (intensity) frequency against diameter as shown in the Figure 2; conversion from the intensity plots to number- or volume-based diameter distribution can be significantly erroneous due to the inherent peak broadening of the intensity distributions.<sup>30</sup> Z-average diameters (i.e. intensity-weighted harmonic mean diameter) were measured, which can be expressed as<sup>31</sup>

$$D_z = \frac{\sum S_i}{\sum \left(\frac{S_i}{D_i}\right)}$$

where  $D_z$  is the z-average diameter,  $S_i$  is the scattered light intensity from particle  $i$  and  $D_i$  is the diameter of particle  $i$ . Polydispersity indexes (PDI) of the two samples were also recorded (Table 1).

For the '30 nm' silver particles, DLS measured diameters of 6 nm (or 20%) larger than the reference value, which may reflect the measurement of a hydrodynamic quantity. A diameter distribution *shift* towards larger sizes is expected owing to a sixth-power dependence of scattered light intensity on the particle diameter.<sup>14</sup> Meanwhile, the PDI shows a narrow diameter distribution for the '30 nm' particles of 11.8 nm in width assuming a Gaussian distribution. However, for the '20 nm' particles there is a vast overestimation of 70% larger in the measured diameter than TEM while the diameter distribution is significantly biased towards larger sizes. Additionally, to eliminate the effect of particle concentration on the measurement accuracy, concentration scaling up was attempted (See SI Section S2). Even so, the sizing results for the '20 nm' sample are in general agreement with other literatures<sup>10-12</sup> where typically an overestimation of over 50% in measured diameter is observed for silver particles of very small diameters (e.g. 10-20 nm). Therefore, the DLS measurements are able to size the '30 nm' sample but not the '20 nm' particles.

**Table 1.** Summary of the sizing results of the four techniques for the '20 nm' and '30 nm'-diameter Ag NPs

and their mixture.

View Article Online

DOI: 10.1039/C8NR09172B

Techniques	Measured Diameters (nm)/ Median Diameters (nm) <sup>a)</sup>	'20 nm'	'30 nm'	'20 + 30 nm'
DLS	Z-average diameter (nm) $d_{\text{intensity median}}$ (nm)	31.1 (PDI = 0.222) <sup>b)</sup> <b><math>31.5 \pm 0.8^b</math></b>	34.7 (PDI = 0.116) <b><math>34.7 \pm 0.2</math></b>	$\times^c$
NTA	Modal diameter(nm) $d_{\text{median}}$ (nm)	$26.6 \pm 8.5$ <b><math>27.8 \pm 0.4</math></b>	$30.0 \pm 6.0$ <b><math>30.4 \pm 0.1</math></b>	$\times$
TEM	Mean diameter (nm) $d_{\text{median}}$ (nm)	$19.0 \pm 4.2$ <b><math>18.5 \pm 0.3</math></b>	$29.2 \pm 4.8$ <b><math>28.9 \pm 0.5</math></b>	-
NI	Mean diameter (nm) $d_{\text{median}}$ (nm)	$19.2 \pm 3.9$ <b><math>18.3 \pm 0.5</math></b>	$30.2 \pm 7.5$ <b><math>28.7 \pm 0.6</math></b>	$\vee^c$

<sup>a)</sup> (' $d_{\text{median}}$ ' means the measured 'median diameters') <sup>b)</sup> (There are two types of standard deviations – the upper-row ones represent the width of the measured diameter distribution (otherwise, PDI is used for DLS results), while the lower-row ones indicate the reproducibility of the median diameters) <sup>c)</sup> (' $\vee$  or  $\times$ ' means being able or not to discriminate the bimodal sample)

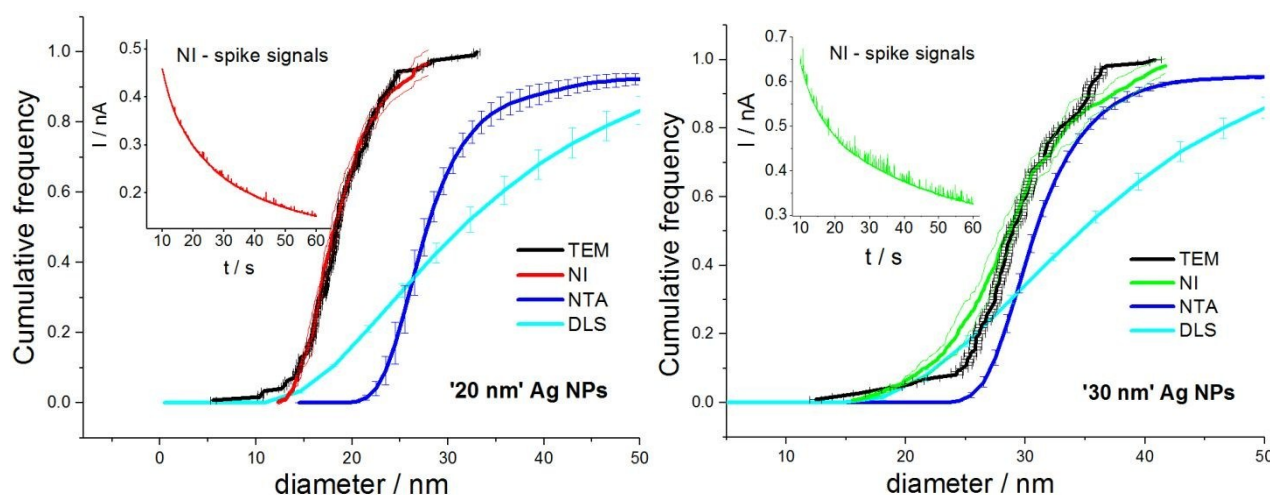


**Figure 2.** Inter-technique sizing comparison in cumulative frequency against diameter for the '20 nm' and '30 nm' silver particles in aqueous dispersions containing 20 mM KCl and 1.8 mM citrate. The inlay figures are chronoamperogram examples (at + 0.8 V vs. Ag/AgCl, duration 60 seconds) with nano-impact (NI) spike signals for oxidation of the 6 pM '20 nm' (red) and '30 nm' (green) silver particles, respectively. Thin lines or error bars alongside the mainstream sizing curves denote the corresponding measure of uncertainty.

### 3.3. Electrochemical measurements

View Article Online  
DOI: 10.1039/C8NR09172B

Having recognized the limited accuracy of the light scattering measurements, we next performed nano-impact (NI) experiments to size the two monomodal samples. A carbon microdisc electrode was immersed in a 20 mM KCl solution containing 6 pM '20 nm' or '30 nm' silver nanoparticles and 1.8 mM citrate. At a step potential of + 0.8 V (vs. Ag/AgCl), five 60-second chronoamperograms were collected each for '20 nm' and '30 nm' silver particles (inlay of Figure 2), where 477 and 1203 spike signals were identified, respectively. The filter design used in this work has been demonstrated to conserve the overall charge transferred in such nano-impact events.<sup>25, 26</sup> The oxidative charge per impact event is converted to the number of silver atoms per particle *via* Faraday's 1<sup>st</sup> law. Specifically, if  $Q$  is the spike charge obtained by integrating current with time and carefully defining a baseline,<sup>22</sup> then

$$Q = Ne$$

where  $e$  is the electronic charge ( $1.60 \times 10^{-19}$  C) and  $N$  is the number of silver atoms in the nanoparticle. This number is independent of the shape of the particle and the technique provides no shape information. However, it is possible to define an 'effective' diameter ( $d$ ) of a perfect sphere containing the same number of atoms and having the same density,  $\rho$  in  $\text{g m}^{-3}$ , as bulk silver ( $10.5 \times 10^6 \text{ g m}^{-3}$ ),

$$\rho = \frac{\frac{N}{N_{Av}} \times A_r(\text{Ag})}{\frac{4}{3} \pi \left(\frac{d}{2}\right)^3}$$

where  $N_{Av}$  is the Avogadro constant and  $A_r(\text{Ag})$  is the relative atomic mass of silver ( $107.9 \text{ g mol}^{-1}$ ). As such, the particle diameter distributions in form of cumulative frequency (i.e. normalized cumulative number of spikes) as a function of diameter were obtained. However, to obtain a 'true'

diameter distribution, the impact data is first windowed to statistically reveal authentic numbers of spikes,<sup>15</sup> and then weighted for diffusion to eliminate the effect of unequal probabilities of detecting the particles owing to their size-dependent mobility (See SI Section S3).<sup>22</sup> As a result, 443 ('20 nm') and 932 ('30 nm') spikes were confirmed as single features and the windowed- and weighted- diameter distributions were depicted in the Figure 2 with measured diameters in Table 1. The thin lines alongside the mainstream, thick sizing curves represent the standard deviations of the experimental reproducibility.

As depicted in Figure 2 (enlarged in Figure 3), the spike height of the '30 nm' impacting particles is observed nearly three times high as that of the '20 nm' sample. This ratio is the same as that for their impact charges, due to the sufficiently fast electrode kinetics at the applied high overpotential ( $\eta = 0.6$  V) and thereof to similar durations of the spikes  $18 \pm 9$  ms ('20 nm') and  $22 \pm 11$  ms ('30 nm'). In terms of impact frequency, it was observed that the smaller '20 nm' particles, however, have a lower impact frequency than the '30 nm' particles. In the diffusion-only regime of particle movements in solution, the flux of NPs towards electrode surface is affected by the size of the particles as discussed above. However, the particles might not be immediately oxidized upon arrival given that the initiation of the oxidation events depends on the quality of electrical contact between the impacting particles and the electrode, which may be largely affected by the surface chemistry of the NPs and the electrolyte condition.<sup>32</sup>

As seen from the Figure 2, the electrochemical measurements show excellent agreement with the TEM reference diameters for both '20 nm' and '30 nm' silver samples. More precisely, the median diameters were measured as  $18.3 \pm 0.5$  nm and  $28.7 \pm 0.6$  nm for the '20 nm' and '30 nm' particles

respectively, which both merely differ by 0.2 nm in diameter from the reference values. To facilitate the comparison of diameter distributions, D10, D25, D50, D75 and D90 percentile values of the TEM and electrochemical sizing curves are used to acquire a measure of accuracy. As a result, the nano-impact diameter distributions are within 2.0% error on average of the TEM results for the '20 nm' particles and within 5.4% error for the '30 nm' particles. In addition, the corresponding standard deviations as from the experimental reproducibility are found to be within less than 3.0% of the average diameters. It is thus concluded that the electrochemical technique provided highly accurate (< 5% error in effective diameters) sizing measurements of these small nanoparticles.

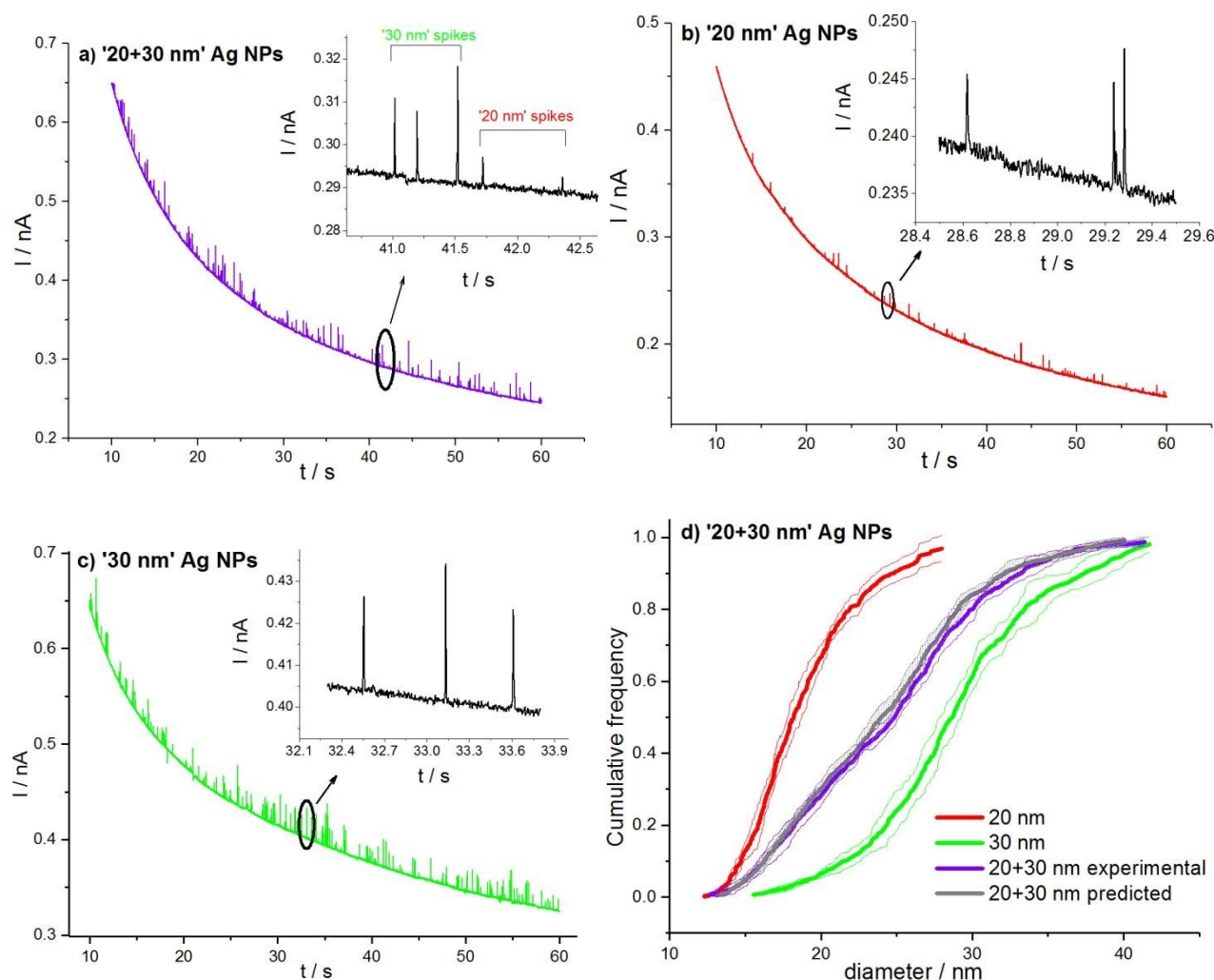


**Figure 3.** a) Chronoamperograms at + 0.8 V vs. Ag/AgCl with a duration of 60 seconds show nano-impact spikes signals for the oxidation of the bimodal sample containing 20 mM KCl and 1.8 mM citrate. The enlarged figure show

concurrent detection of the two distinct kinds of spikes. Similarly, the spike data are presented for the individual b) '20 nm' and c) '30 nm' samples. d) Nano-impact sizing curves for the individual '20 nm' (red), '30 nm' (green) particles, the mixed '20+30 nm' (violet) sample and the predicted diameter distribution for the mixture (gray). Thin lines alongside each thick curve denote the standard deviation of the measured diameters.

View Article Online  
DOI: 10.1039/C8NR09172B

Building on the success of the accurate sizing of the individual NP dispersions, the nano-impact technique was further applied to size a bimodal sample of a mixture of the '20 nm' and '30 nm' Ag NPs. The carbon microdisc electrode was immersed in the 20 mM KCl solution containing deliberately mixed 6 pM '20 nm' and 6 pM '30 nm' silver nanoparticles with 1.8 mM citrate. Under the same conditions, five chronoamperograms were collected with 1391 spikes and then after windowing 1234 spikes. Figure 3c shows one chronoamperogram with nano-impact spikes for the bimodal sample. For ease of comparison, examples of the spikes for the individual samples are provided in Figure 3a& 3b. The impact frequencies of the '20 nm', '30 nm' and mixed '20+30 nm' particles are  $1.5\text{ s}^{-1}$ ,  $3.1\text{ s}^{-1}$  and  $4.1\text{ s}^{-1}$ , respectively. The cumulative frequency as a function of diameter is plotted as shown in Figure 3d for the three experimental cases and the predicted mixture which is derived from the frequency-weighted sum of the two individual sizes.

Figure 3 show that the two kinds of spikes for the individual '20 nm' and '30 nm' samples are observed together in the chronoamperograms of the bimodal sample. The measured diameter distribution lies in the middle of the two sizing curves for the individual samples with a median diameter of  $24.8 \pm 0.5\text{ nm}$ . An excellent agreement between the experimental curve and the predicted is observed. More precisely, by comparing the five D10-90 percentile values of the two diameter distributions for the mixture, the experimental results show an error of less than 2.0% of the predicted. In terms of impact frequency, although the '30 nm' sample rather than the bimodal

sample appears to have the most spike signals, statistical analysis based on a Poisson distribution (See SI Section S3) reveals a number of 27% fewer single impact events by the data windowing as it was observed that many spikes came out so close that they are considered as single impact events composed of multiple collisions. Consequently, the '30 nm' sample actually has a lower impact frequency than the bimodal sample, and the measured and predicted impact frequencies, as being 4.1 and 4.6 s<sup>-1</sup> respectively are consistent. It is concluded that the electrochemical detection and sizing measurements are able to discriminate two 10-nm-different sizes in high accuracy and are thereof essentially independent of the particle size polydispersity.

In terms of the measurement principle, nano-impacts have advantages over the other techniques to efficiently provide accurate information on particle sizes. It is highlighted that the electrochemical technique is a volume-based method as it *in situ* measures the total number of electrons transferred of each single particle upon collision at the electrode-solution interface. Subsequently, the charge data is, regardless of the particle shape, converted to a precise number of constituent atoms thus giving its effective diameter for a perfect sphere containing the same number of atoms ( $Q \propto d^3$ ). This, therefore, serves as a solid basis of discriminating particles of very similar sizes. One major requirement for such precise size determination is complete electrolysis of nanoparticles at the three phase boundary formed on impacts. Depending on the particle identity, this requires identification of suitable electrolyte species and their concentrations and the necessary potential applied. Specifically, previous research shows, under those conditions, an upper sizing limit of *ca.* 50 nm for silver NPs<sup>33</sup> but that 100 nm-diameter AgCl NPs can be readily sized.<sup>34</sup> To date, many metallic NPs (e.g. Cu,<sup>35</sup> Ni,<sup>36, 37</sup> Au<sup>38, 39</sup>), metal salt NPs (e.g. AgCl,<sup>34</sup> Hg<sub>2</sub>Cl<sub>2</sub><sup>40</sup>), organic NPs (e.g. indigo<sup>17</sup>) and polymeric NPs (e.g. poly(*N*-vinylcarbazole)<sup>18</sup>) have been shown to



undergo complete oxidation or reduction, or oxidative doping respectively, allowing accurate nano-impact sizing of themselves.

[View Article Online](#)  
DOI: 10.1039/C8NR09172B

As to TEM measurements, size information tends to be skewed by the significant assumption based on 2D cross-section images especially for the particles with high irregularity. To obtain true volumes, electron tomography is required.<sup>15</sup> DLS and NTA techniques quantifying particulate diffusional movements in bulk are only able to measure hydrodynamic radii based on the Stoke-Einstein law assuming equivalent diffusing perfect spheres. They are unable to provide any related shape information. DLS is complex to interpret for non-spherical particles because of the need to quantify the contribution of rotational diffusion, although the electric birefringence methods can offer size distributions of non-spherical particles if a shape is assumed.<sup>41</sup> Also in many cases, the precise difference between a particle's hydrodynamic diameter and geometric diameter is difficult to know considering the uncertain effects of the often used capping agents in NP systems. It is also well known that DLS can only resolve a diameter difference of two particles of at least a factor of 3, and even in presence of tiny portions (e.g. 5%) of larger particles smaller NPs are not possible to be detected;<sup>7, 42</sup> NTA heavily relies on a short-wavelength laser for smaller particles that is often inaccessible, both of which essentially root in the intrinsic scattering principle of these techniques. Therefore, especially in the case of sizing small, multimodal NPs, nano-impacts largely excel the light scattering techniques.

## 4. Conclusions

Accurate NTA sizing measurements require a shorter-wavelength 405 nm laser for the detection of the individual '30 nm' silver particles, while DLS shows biased diameter distributions for these particles towards larger sizes with 20% overestimation in diameter. Neither light scattering technique is able to accurately size the smaller '20 nm' particles. Moreover and fundamentally,

these techniques only measure in hydrodynamic terms neglecting any shape information. In contrast, nano-impacts accurately measure geometric diameters in terms of the number of constituent atoms for *both* '20 nm' and '30 nm' particles. This electrochemical technique has further revealed its advantages as a volume-based method that is able to resolve these similar sizes in high accuracy, whereas due to inherent limitations of light scattering measurements this is not possible for the DLS and NTA. On these bases, we conclude that the nano-impact technique is an alternative, accurate way of sizing both nearly mono- and poly-disperse NP samples in the small-size range; particles as small as 5 nm have been successfully sized.<sup>25</sup>

## Acknowledgements

The authors are grateful to Dr. Tom Dennison and Mr. Liam Cole of Malvern Analytical for the kind help in the NTA measurements with the 405 nm laser. This project is sponsored by the funding from the European Research Council (ERC) under the European Union's Seventh Framework Programme (FP/207-2013), ERC Grant Agreement no. 320403.

## References

1. K. L. Kelly, E. Coronado, L. L. Zhao and G. C. Schatz, *Journal of Physical Chemistry B*, 2003, **107**, 668-677.
2. X. Zhou, W. Xu, G. Liu, D. Panda and P. Chen, *Journal of the American Chemical Society*, 2009, **132**, 138-146.
3. S. Kim and D. Y. Ryu, *Journal of Applied Toxicology*, 2013, **33**, 78-89.
4. F. Laborda, E. Bolea, G. Cepriá, M. T. Gómez, M. S. Jiménez, J. Pérez-Arantegui and J. R. Castillo, *Analytica chimica acta*, 2016, **904**, 10-32.
5. M. Gaumet, A. Vargas, R. Gurny and F. Delie, *European journal of pharmaceuticals and biopharmaceutics*, 2008, **69**, 1-9.

6. S. K. Brar and M. Verma, *TrAC Trends in Analytical Chemistry*, 2011, **30**, 4-17.
7. V. Filipe, A. Hawe and W. Jiskoot, *Pharmaceutical research*, 2010, **27**, 796-810. View Article Online  
DOI: 10.1039/C8NR09172B
8. F. Meli, T. Klein, E. Buhr, C. G. Frase, G. Gleber, M. Krumrey, A. Duta, S. Duta, V. Korpelainen and R. Bellotti, *Measurement Science and Technology*, 2012, **23**, 125005.
9. P. Eaton, P. Quaresma, C. Soares, C. Neves, M. de Almeida, E. Pereira and P. West, *Ultramicroscopy*, 2017, **182**, 179-190.
10. M. Ahamed, R. Posgai, T. J. Gorey, M. Nielsen, S. M. Hussain and J. J. Rowe, *Toxicology and Applied Pharmacology*, 2010, **242**, 263-269.
11. S. A. Cumberland and J. R. Lead, *Journal of chromatography A*, 2009, **1216**, 9099-9105.
12. G. Singhal, R. Bhavesh, K. Kasariya, A. R. Sharma and R. P. Singh, *Journal of Nanoparticle Research*, 2011, **13**, 2981-2988.
13. D. Langevin, O. Lozano, A. Salvati, V. Kestens, M. Monopoli, E. Raspaud, S. Mariot, A. Salonen, S. Thomas and M. Driessen, *Nanoimpact*, 2018, **10**, 97-107.
14. H. Moosmüller and W. P. Arnott, *Journal of the Air & Waste Management Association*, 2009, **59**, 1028-1031.
15. C. A. Little, C. Batchelor-McAuley, N. P. Young and R. G. Compton, *Nanoscale*, 2018, **10**, 15943-15947.
16. Y. G. Zhou, N. V. Rees and R. G. Compton, *Angewandte Chemie*, 2011, **123**, 4305-4307.
17. W. Cheng, X. F. Zhou and R. G. Compton, *Angewandte Chemie*, 2013, **125**, 13218-13220.
18. X. F. Zhou, W. Cheng and R. G. Compton, *Angewandte Chemie*, 2014, **126**, 12795-12797.
19. S. V. Sokolov, S. Eloul, E. Kätelhön, C. Batchelor-McAuley and R. G. Compton, *Physical Chemistry Chemical Physics*, 2017, **19**, 28-43.
20. K. J. Stevenson and K. Tschulik, *Current Opinion in Electrochemistry*, 2017, **6**, 38-45.
21. T. Albrecht, S. Horswell, L. Allerston, N. Rees and P. Rodriguez, *Current Opinion in Electrochemistry*, 2017, **7**, 138-145.
22. C. A. Little, R. Xie, C. Batchelor-McAuley, E. Kätelhön, X. Li, N. P. Young and R. G. Compton, *Physical Chemistry Chemical Physics*, 2018, **20**, 13537-13546.
23. Y. Wan, Z. Guo, X. Jiang, K. Fang, X. Lu, Y. Zhang and N. Gu, *Journal of colloid and interface science*, 2013, **394**, 263-268.
24. J. C. Lees, J. Ellison, C. Batchelor - McAuley, K. Tschulik, C. Damm, D. Omanović and R. G. Compton, *ChemPhysChem*, 2013, **14**, 3895-3897.
25. C. Batchelor-McAuley, J. Ellison, K. Tschulik, P. L. Hurst, R. Boldt and R. G. Compton, *Analyst*, 2015, **140**, 5048-5054.

26. E. Kätelhön, E. E. Tanner, C. Batchelor-McAuley and R. G. Compton, *Electrochimica Acta*, 2016, **199**, 297-304. View Article Online  
DOI: 10.1039/C8NR09172B
27. Whilst the commercial working electrode is labelled as 33  $\mu\text{m}$  in diameter, on calibration it exhibits  $39.8 \pm 0.6 \mu\text{m}$ . The measured value is later used in calculation of theoretical diffusion flux for the NPs.
28. R. LeBel and D. Goring, *Journal of Chemical and Engineering Data*, 1962, **7**, 100-101.
29. In the TEM data analysis, a freehand tool in the ImageJ software was used to draw boundaries along the particle edges in the 2D images. As without any restrictions on the drawn shape it allows precise particle area to be measured.
30. M. Dionzou, A. Morère, C. Roux, B. Lonetti, J.-D. Marty, C. Mingotaud, P. Joseph, D. Goudounèche, B. Payré and M. Léonetti, *Soft Matter*, 2016, **12**, 2166-2176.
31. (1) International Standard ISO13321 Methods for Determination of Particle Size Distribution Part 8: Photon Correlation Spectroscopy, International Organisation for Standardisation (ISO) 1996. (2) International Standard ISO22412 Particle Size Analysis – Dynamic Light Scattering, International Organisation for Standardisation (ISO) 2008.
32. K. Ngamchuea, R. O. Clark, S. V. Sokolov, N. P. Young, C. Batchelor - McAuley and R. G. Compton, *Chemistry-A European Journal*, 2017, **23**, 16085-16096.
33. C. A. Little, X. Li, C. Batchelor-McAuley, N. P. Young and R. G. Compton, *Journal of Electroanalytical Chemistry*, 2018, **823**, 492-498.
34. T. R. Bartlett, S. V. Sokolov and R. G. Compton, *ChemistryOpen*, 2015, **4**, 600-605.
35. B. Haddou, N. V. Rees and R. G. Compton, *Physical Chemistry Chemical Physics*, 2012, **14**, 13612-13617.
36. E. J. Stuart, Y.-G. Zhou, N. V. Rees and R. G. Compton, *Rsc Advances*, 2012, **2**, 6879-6884.
37. Y.-G. Zhou, B. Haddou, N. V. Rees and R. G. Compton, *Physical Chemistry Chemical Physics*, 2012, **14**, 14354-14357.
38. A. L. Suherman, G. Zampardi, S. Kuss, E. E. Tanner, H. M. Amin, N. P. Young and R. G. Compton, *Physical Chemistry Chemical Physics*, 2018, **20**, 28300-28307.
39. D. Qiu, S. Wang, Y. Zheng and Z. Deng, *Nanotechnology*, 2013, **24**, 505707.
40. T. R. Bartlett, C. Batchelor-McAuley, K. Tschulik, K. Jurkschat and R. G. Compton, *ChemElectroChem*, 2015, **2**, 522-528.
41. P. Arenas-Guerrero, Á. V. Delgado, K. J. Donovan, K. Scott, T. Bellini, F. Mantegazza and M. L. Jiménez, *Scientific Reports*, 2018, **8**, 9502.

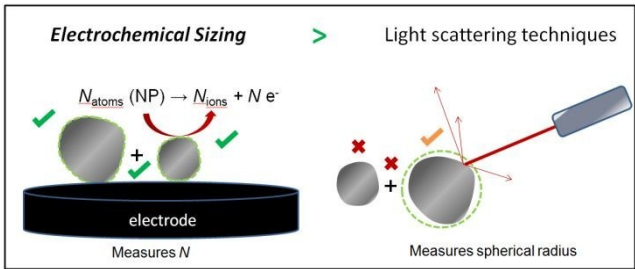
42. E. Tomaszewska, K. Soliwoda, K. Kadziola, B. Tkacz-Szczesna, G. Celichowski, M. Cichomski, W. Szmaja and J. Grobelny, *Journal of Nanomaterials*, 2013, **2013**, 60.

[View Article Online](#)

DOI: 10.1039/C8NR09172B

ToC figure:

View Article Online  
DOI: 10.1039/C8NR09172B



**ToC text:** Electrochemical sizing of nanoparticles via particle impacts size smaller particles than optical methods.